7-1997

Electro-Optical Study of Nematic Elastomer Gels

C.C. Chang

Liang-Chy Chien
Kent State University - Kent Campus, lchien@kent.edu

R. B. Meyer

Electro-optical study of nematic elastomer gels

C.-C. Chang,[1] L.-C. Chien,[2] and R. B. Meyer[1]
[1]*The Martin Fisher School of Physics, Brandeis University, Waltham, Massachusetts 02254-9110*
[2]*Liquid Crystal Institute, Kent State University, Kent, Ohio 44242*
(Received 6 December 1996)

We report on an electro-optical study of a liquid-crystal–polymer composite system. This system is made by dissolving a small amount of acrylate monomers (8%) plus crosslinkers in a nematic liquid crystal, and then photopolymerizing the homogeneous mixture. These nematic gels show properties different from those of ordinary nematics or polymer stabilized liquid crystals. By studying the electric field induced Frederiks transition, some basic properties of the nematic gels can be deduced. We compare the experimental results to a simple phenomenological model of the nematic gel, involving a characteristic length scale of order 1 μm, which is also visible as speckles, an effective internal aligning field of a few statvolts per cm, and an increased rotational viscosity on the order of 10^4 P. We indicate how a microscopic model might relate the first two of these parameters. [S1063-651X(97)07707-6]

PACS number(s): 61.30.−v, 78.20.Jq, 82.70.Gg

The liquid-crystal–polymer composite materials were introduced more than one decade ago. These systems combine the anisotropic properties of thermotropic liquid crystals and the rigidity of polymer networks. Two examples of this kind are ''polymer dispersed liquid crystals'' (PDLC) [1] and ''polymer stabilized liquid crystals'' (PSLC) [2]. For PSLC, side chain monomers are usually used. One example is putting a few percent ($\sim$ 1–5 wt %) of diacrylate monomers in the liquid crystal, then photopolymerizing the homogeneous mixture. The resulting polymer network can provide a memory effect in which it locks in the structure defined by a combination of the boundary conditions on the director provided by solid surfaces and an external field applied during the photopolymerization. In the case of strong anchoring, most of the mesogenic moieties will follow the director and the polymer main chains will tend to be perpendicular to the director. This point has been confirmed by x-ray studies [3].

Even though the two systems show promising aspects in terms of applications, they have an important feature in common which makes them difficult to characterize: they are highly phase separated on a microscopic scale, so that their average physical properties depend on the details of the phase separation which occurs during polymerization. Often, in PSLC systems the phase separation is visible on a micrometer (or larger) scale, and can be roughly described as a network of macroscopic polymer strands or fibrils, subdividing the liquid crystal into a set of multiply connected micrometer-sized compartments. Within each compartment, there is relatively pure liquid-crystal material, and the mean orientation of the nematic director is roughly preserved from compartment to compartment. In this paper, a different system is studied: We believe that we can prepare a homogeneous gel in a nematic liquid crystal, formed from a mixture of nematic liquid crystal plus nematiclike acrylate monomers. During the polymerization, our model picture is that a multiply connected gel network of single polymer chains forms throughout the nematic without phase separation. This leads to an intimately connected system of polymer and nematic, with new properties arising from the interaction of the two component systems. We have chosen to study a composition at which the rigidity of the polymer network is important but not completely dominant, so that the nematic director still responds to weak externally applied fields.

The nematic liquid crystal K15 (I) (EM Chemicals) was used. Then acrylate monomer 4′-(4-acryloylbutyloxy)-4-cyanobiphenyl (II) (8%) was added to the K15, as was diacrylate monomer 4,4′-bisacryloyl-biphenyl (III) (0.8%) for crosslinking. A small amount of photoinitiator, benzoin methyl ether, was also added to the mixture. The concentration of the diacrylate crosslinking monomer was adjusted to its minimum value so that the system gelled, but the gross nonuniformity found in PSLC systems due to phase separation could be eliminated,

$$CH_3-(CH_2)_4-C_6H_4-C_6H_4-CN \quad \text{(I)},$$

$$CH_2=CH-CO_2-(CH_2)_4-O-C_6H_4-C_6H_4-CN \quad \text{(II)},$$

$$CH_2=CH-CO_2-C_6H_4-C_6H_4-O_2C-CH=CH_2 \quad \text{(III)}.$$

This nematic gel showed a fairly uniform texture when observed with the polarizing microscope, although after gelation slight speckles on the few-micrometer scale are visible between crossed polarizers. As discussed at the end of the paper, we interpret these speckles not as phase separation, but as evidence for a static random internal torque field produced by the intrinsic inhomogeneities of the polymer network. This internal random field leads to slight misalignments of the nematic director on a length scale that results from competition between the disorienting effects of the random field and the smoothing effects of the nematic elasticity. By rotating the sample between crossed polarizers, one could see that the speckles represented local misorientations of the director by a few degrees.

The nematic mixture was sandwiched between two indium-tin-oxide (ITO) coated glass slides separated by either Mylar or Teflon spacers. The plates were coated with polyvinyl alcohol and rubbed unidirectionally so that a planar nematic cell could be achieved. Then the cell was placed under an UV lamp for a couple of hours to make sure that the

monomers had reacted completely. The alignment of this system still depends on the anchoring force from the surfaces. For a thin sample $d \sim 20$ μm, the cell remained clear after the photopolymerization, which means that the anchoring force is strong enough to preserve the orientation of nematic gels. Because of the surface alignment and the nematic ordering, the mesogenic groups remain parallel to the director, while the polymer main chains will have preferential orientation perpendicular to the director. Once the sample becomes very thick ($d \sim 100$ μm), overall orientation is harder to preserve during polymerization. Because the anchoring force is weaker in a thick sample, certain parts of the sample became turbid after the photopolymerization, possibly due to transient heating and flow effects induced by the chemical reactions. Applying a strong magnetic field along the rubbing direction during the polymerization can be helpful to maintain alignment during polymerization.

The conoscopic method was used to study this system. It is known that by illuminating a planar nematic cell placed between crossed polarizers, such that the rubbing axis, defining the unperturbed director of the nematic, is at 45° relative to the polarizer and the analyzer, interference patterns can be observed as a result of the phase difference between the ordinary and extraordinary waves. The interference patterns contain two sets of dark hyperbolas, which are characteristic of a uniaxial slab of material with its optical axis in one direction parallel to the surface of the slab. For normal incidence (at the center of the conoscopic image), the transmitted light intensity in the absence of an applied field can be described as $I \propto \sin^2[\pi d(n_e - n_o)/\lambda]$, where n_o and n_e are the ordinary and the maximum extraordinary indices of refraction, respectively, and λ is the wavelength of the incident light. By applying an electric field and rotating the director, the effective birefringence changes, and the interference patterns move. The extraordinary wave path length decrease δ, in units of the optical wavelength, induced by an electric field can be defined as $\delta = d(n_e - n_{\text{eff}})/\lambda$ in which n_{eff} is the extraordinary index averaged over the sample thickness. By observing how the interference patterns change under the influence of an electric field, some basic properties of this system can be understood [4].

Suppose the rubbing axis of a planar nematic cell is along the x direction. By applying an ac electric field in the z direction, the director will tilt in the xz plane and splay-bend patterns can be generated. The equilibrium torque equation can be derived from nematodynamics:

$$K\frac{d^2\psi}{dz^2} + \frac{D_z^2}{4\pi}\frac{\epsilon_a \sin\psi\cos\psi}{(\epsilon_\parallel \sin^2\psi + \epsilon_\perp \cos^2\psi)^2} = 0, \qquad (1)$$

where $\psi(z)$ is the tilt angle relative to the x axis, $K(=K_1=K_3)$ the elastic constant, $\epsilon_a(=\epsilon_\parallel - \epsilon_\perp)$ the dielectric anisotropy, and D_z the z component of the electric displacement field. Solving for $\psi(z)$, and then calculating n_{eff}, one can show that δ should depend linearly on $V - V_c$ when V is just above V_c, where V_c is the threshold voltage for the Frederiks transition [5].

A HeNe laser (Melles Griot, $\lambda = 0.633$ μm) which generates linearly polarized light was used as the monochromatic light source. The light passed through a spatial filter and a high power lens (50×, numerical aperture equal to 0.85) so that a clean divergent beam was achieved. The position of the sample was right after the high power lens and in front of an analyzer. A screen was put behind the analyzer so that the interference patterns could be observed. A function generator and transformer were used together to generate ac voltages with frequency of 1 kHz.

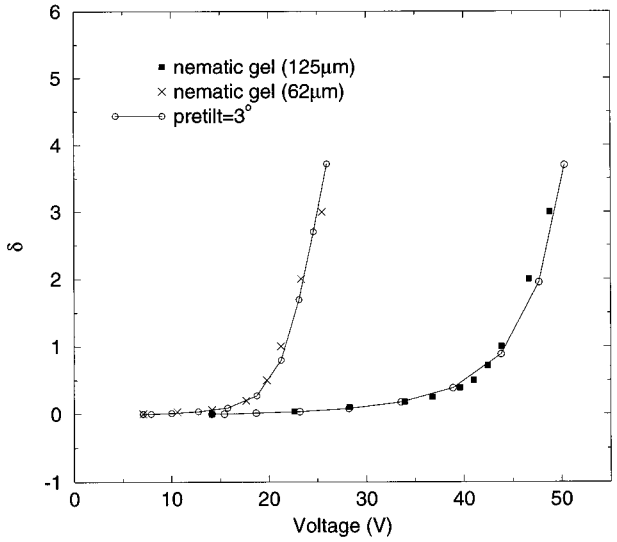

FIG. 1. Comparisons of the theoretical calculations and the experimental data with the fitting parameters $d' = 1.3$ and 1.2 μm, $V_0 = 14.1$ and 7.1 V, for the 125 and 62 μm cells, respectively.

The experiments were done with cells of nematic gels of two different thicknesses, 62 and 125 μm. Even though a fine speckle pattern was observed after polymerization, the samples, nevertheless, were more uniform than the typical PSLC cell and quantitative measurements were obtained for certain areas of the cells. By using the optical method described above, several observations were made. (1) Without the presence of an electric field, two sets of hyperbolas still showed up on the screen with uniaxial symmetry just like those patterns seen in the case of ordinary nematics. (2) Compared to ordinary nematics, the patterns did not move until a much higher voltage was applied, and this threshold voltage was larger for thicker samples. (3) Even though the patterns did move, they always kept uniaxial symmetry, rather than shifting in one direction as in the ordinary nematics. (4) For any given point on the screen, even as voltage increased to a high level, there were only a few interference fringes that moved past that point, which was far less than in the ordinary nematic. (5) Once the interference patterns started to move, the δ-V relationship did not support the linearity seen in the ordinary nematics. (6) At very high voltage, the interference pattern became blurry.

The results of the phase difference measurements vs applied voltage are shown in Fig. 1. The samples were first moved around until the hyperbolas formed an ''X'' at the center of the screen, thus selecting a point for which $d\Delta n/\lambda =$ integer. Applied voltages were recorded each time the dark hyperbolas formed an ''X'' again. There existed a certain degree of error because the interference patterns became blurry when larger voltages were applied. By using a photodiode with a small iris diaphragm in front of the center of the ''X,'' the intensity change can be monitored and be converted to phase difference by using the relation

TABLE I. Parameters used in the theoretical calculations.

$\epsilon_{\parallel}$	$\epsilon_{\perp}$	n_e	n_o	K	λ	d
20.0	7.0	1.74	1.54	8.0×10^{-7} dyn	0.633 μm	124.0 μm

$I\sim \sin^2(\pi\delta)$. This method is useful, especially for small δ.

In order to explain the experimental observations, we introduce a simple phenomenological model for the effects of the gel. Several modifications have to be introduced into the ordinary theory of the Frederiks transition: (1) There must exist a characteristic length scale d' for the material, which is different from the length scale of ordinary nematics ($=d$, the thickness of the sample). The high voltages needed indicate that d' is very small. For each layer of thickness d', the threshold field is equal to E_c for the Frederiks transition. Then V_c will depend linearly on d. (2) There should be a constraint coming from the gel structure and its orientation should be along the original director. The polymer network produces a mean orienting effect described as an effective internal field E_0 applied along the director. One can easily calculate V_c from the consideration of the contribution of the effective internal field to the free energy:

$$V_c=\left(V_0^2+4\pi^3\frac{d^2}{d'^2}\frac{K}{\epsilon_a}\right)^{1/2}, \tag{2}$$

where $V_0(=E_0d)$ can be used as a representation of the network constraint and can be measured experimentally. (3) Because the interference patterns showed uniaxial symmetry even with the presence of the applied voltages, there must be equal thicknesses of the sample tilted in the $+\hat{\mathbf{z}}$ and $-\hat{\mathbf{z}}$ directions. The simplest model is a stack of layers of thickness d', with the director alternating its tilt direction from layer to layer. $\psi(z)$ then can be described as $\sin(\pi z/d')$ for small deformations. This along with (1) predicts that the relaxation time of the nematic gels is dependent only on d', but not on the sample thickness d. Because of these mixed orientations which are not really homogeneous thin layers, at higher voltages the birefringence decreases and lots of scattering occurs, which is why the patterns became blurry. The small value of d' means that the V_c is large. Therefore only a few fringes move across the sample before it becomes too blurry for further measurements. (4) The nonlinearity of the δ-V curves suggests that there is pretilt of the director in the many effective thin layers we imagine existing in the system, as another effect of the polymer network. Gels are well known to be slightly inhomogeneous, and we certainly see speckles representing local director misorientations of a few degrees.

In order to understand how the pretilt angle can affect the phase difference, numerical simulation of an ordinary nematic based on Eq. (1) was done. For any given D_z, which is a constant, $\psi(z)$ can be calculated for the equilibrium condition. Then the δ-V relationship can be understood. Table I lists the parameters used in the calculations. The results of calculations are shown in Fig. 2 for three different pretilt angles for the 124 μm cell. Similar calculations can be done for the 62 μm cell. In an ordinary nematic cell, there is only one layer with the length scale d and no constraint from the network, which means $V_0=0$. In the normal Frederiks transition, $\psi(z)$ is always zero when V is smaller than V_c. This is not true when the system has a pretilt. In that case, the electric torque is never zero and $\psi(z)$ will increase even with the presence of a small field. This results in a nonzero δ for any applied voltage. The change of δ is small for small V, and becomes larger when V is comparable to V_c. This can easily be observed in Fig. 2. By comparing the results shown in Fig. 2 with the experimental data shown in Fig. 1, qualitative agreement can be found. Then the idea of the internal field can be put into the calculations. This field constrains the liquid-crystal molecules to align along the direction defined by the network, when the applied voltage is below V_0. When V is greater than V_0, $|\psi(z)|$ starts to increase slowly, due to the pretilt, and interference fringes start to move.

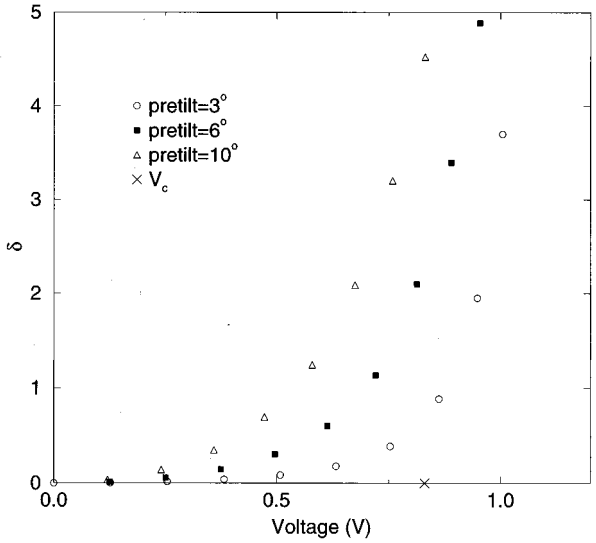

FIG. 2. Calculated δ as a function of three different pretilt angles for a 124 μm sample. The threshold voltage ($V_c=0.83$ V) is represented as $\times$ in the figure.

The results of calculations can be used to fit the experimental data shown in Fig. 1 because δ is proportional to the overall sample thickness. Two fitting parameters for the data above V_0 can be adjusted here: the pretilt angle and the characteristic length scale d'. The voltages can be rescaled in order to fit the experimental data by using the following function:

$$V=\left(V_0^2+\frac{d^2}{d'^2}V_{\mathrm{cal}}^2\right)^{1/2}, \tag{3}$$

where d/d' represents the number of effective layers in the sample and V_{cal} is the voltage from the calculations shown in Fig. 2. V_0 is the voltage representing the internal constraint, which is equal to 14.1 and 7.1 V for the 125 and the 62 μm cells, respectively.

The results of fitting are shown as the solid lines in Fig. 1. Both experimental data sets have the best fits for a pretilt angle equal to 3°, consistent with our observations of speckles. The characteristic lengths d' are chosen to be 1.3 and 1.2 μm for the 125 and the 62 μm cells, respectively. The threshold voltages V_c [from Eq. (2)] can then be calculated

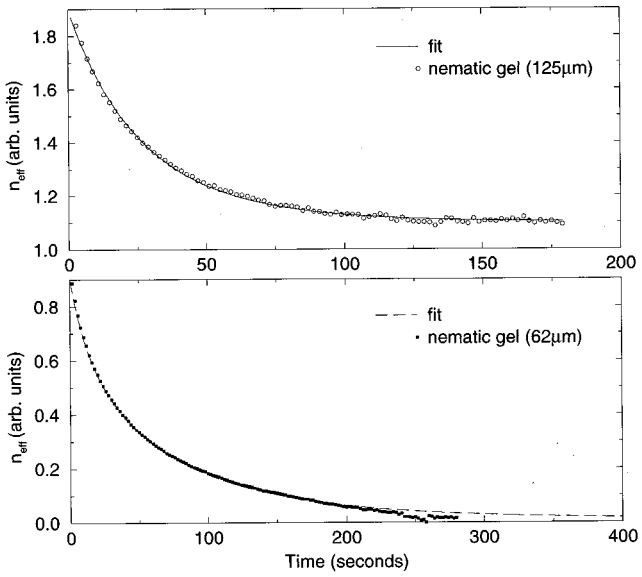

FIG. 3. Experimental results of measurements of n_{eff} for nematic gels as a function of time for the 125 and 62 μm cells. Note that the data for the 62 μm cell are far away from a simple exponential decay and it takes even longer to relax than the 125 μm cell. The fitting curves are the results of model calculations explained in the text.

to be 42.3 and 23.4 V. These values may vary for different samples, or even for different spots within the same sample, due to large scale nonuniformity in gelation.

One major hypothesis of the model is to propose that there exists a characteristic length scale d'. One way of testing this hypothesis is to measure the relaxation time of the system. In our model, the dynamic equation can be written as

$$K\frac{\partial^2\psi}{\partial z^2}-\frac{\epsilon_a}{4\pi}E_0^2\sin\psi\cos\psi=\gamma_1\frac{\partial\psi}{\partial t} \tag{4}$$

when the applied electric field is removed at $t=0$. For small deformations, the time dependent part of ψ will be proportional to $\exp(-t/\tau)$, where $\tau=\gamma_1/[K\pi^2/d'^2+\epsilon_a V_0^2/(4\pi d^2)]$ is the relaxation time of the nematic gels.

One way of measuring the relaxation time is to apply a voltage and then to ground both ITO electrodes at $t=0$ and monitor how the intensity changes with time. The intensity is proportional to the square of a sinusoidal function. The only time dependent component is from n_{eff}, the average index of refraction of the extraordinary wave. For small director deformations $n_{\mathrm{eff}}(t)\sim\psi^2\sim\exp(-2t/\tau)$. By monitoring the time dependent part of the intensity, one can then measure the relaxation time of the system.

The results of experimental measurements are shown in Fig. 3 for the 125 and the 62 μm cells, respectively. The data for the 125 μm cell are close to an exponential function. The argument that there exists a small variation of d' relative to the mean characteristic length can be put into the model, to fit the remaining small deviations observed in the data. One way of describing this variation is to expand the time dependent part of n_{eff} for small ψ:

$$n_{\mathrm{eff}}\sim\int_0^d\psi^2dz=d\sum_i P(d_i')\exp\left(-2\frac{t}{\tau(d_i')}\right), \tag{5}$$

where $P(d_i')$ is the probability for the characteristic length d_i'. Assuming a Gaussian distribution, $P(d_i')\sim\exp[-(d_i'-\overline{d'})^2/(2\sigma^2)]$, where $\overline{d'}$ is the mean length scale which is determined to be 1.3 μm from the fitting result of Fig. 1, and σ is the standard deviation. By putting τ into Eq. (5), the experimental data can be fitted by choosing σ to be 0.2 μm and γ_1 to be 2.2×10^4 P. The solid line represents the best fit of the experimental data. The average τ can be calculated to be 57 s, which is much larger than the time constant of K15 ($\sim$16 s) for the same sample thickness. This long relaxation time is also different from that of a PSLC formed with fibrils of polymer and pockets of liquid crystal. In that case, small volumes of pure nematic, under the orienting influence of the surrounding polymer fibrils, would relax extremely quickly.

For the cell of thickness 62 μm, the above argument alone cannot explain the experimental data. There are at least two time scales existing in the measurements of n_{eff}. One possible explanation is that because of the large scale nonuniformity in gelation of the sample, there are areas with two different values of γ_1 in the part of the sample we observed. For some areas with more polymer, γ_1 is larger; for some areas with more free liquid-crystal molecules, γ_1 is smaller. The equilibrium solution $\psi(z)$ from Eq. (1) for small D_z was then used as the initial condition for Eq. (4), and how $\psi(z)$ relaxed with time was monitored. The value of n_{eff} was recorded when δ was smaller than 1/2. The value of E_0 in Eq. (4) is equal to 3.8 statvolts/cm for the nematic gel used in the experiment.

The results of calculations were rescaled in both axes to fit the experimental data. The fitting curve is shown as the dashed line in Fig. 3. The remaining difference between the fitting curve and the experimental data could come from a distribution of the characteristic lengths. The scaling in the time axis is related to the two values of γ_1, which can then be calculated to be 1.1×10^4 and 6.4×10^4 P. They have the same order of magnitude as the rotational viscosity for the 125 μm cell described earlier. This order of magnitude is in the range of that for similar systems reported by others [6,7].

Although the results we present here concern only one sample composition, and our model for analyzing them is purely phenomenological, we believe that this may serve as a starting point for more thorough consideration of this kind of gelled liquid-crystal–polymer system. The effective length scale and internal field that we hypothesize to fit the data might be related to a microscopic model of polymer–liquid-crystal interactions. We picture the following scenario relating these two features of our model.

First, the polymer network is formed in the nematic phase, and therefore preserves the anisotropic structure of that phase, so it has a mean orientation. However, the polymerization process is not entirely uniform, and local misorientations, relative to the director, are created on a variety of length scales, with long wavelength fluctuations being suppressed by the nematic alignment. Note that the intrinsic length scale between crosslinks in the gel should be on the order of 10 nm, much smaller than our observed d' of about

1 μm. The question is why we see the dominant fluctuations at a length scale much larger than that of the polymer network. One answer could be macroscopic phase separation, but we picture a different mechanism.

Once the polymer is formed, it acts as an internal field $\vec{E}_{\rm int}$ which has a uniform part corresponding to E_0 in our model, in the x direction, and a small random part $\vec{E}_\perp$ in the y and z directions. In the free energy density, the director is coupled to this effective field by a term $f_p = -(\epsilon_a/8\pi)[\hat{n}\cdot(E_0\hat{x}+\vec{E}_\perp)]^2$. The mean director is parallel to E_0, but static distortions of the director field, $\vec{n}_\perp$, are driven by $\vec{E}_\perp$. Fourier analyzing $\vec{n}_\perp$ and $\vec{E}_\perp$, one finds that for wave vector q, $n_\perp(q)\sim[E_0E_\perp(q)]/(E_0^2+4\pi Kq^2/\epsilon_a)$. For $E_\perp(q)$ an increasing function of q, this produces a spectrum of $n_\perp(q)$ that is peaked at $q\simeq E_0\sqrt{\epsilon_a/(4\pi K)}$. For our value of E_0, this gives a wavelength for the dominant fluctuations of $\vec{n}_\perp$ of $\lambda\simeq 15$ μm.

The exact peak wavelength depends on the form of $E_\perp(q)$, and our measured d' should be comparable to $\lambda/2$. Basically the nematic elasticity prevents the director from following the shortest wavelength components of $E_\perp$. In our measurements, wavelengths below about 1 μm are suppressed, even though $E_\perp$ should have significant components down to wavelengths of about 10 nm.

Our overall approach to data analysis here emphasizes looking for a few parameters that describe the quantitative measurements, consistent with the qualitative observations. It is somewhat surprising that a single length scale and a few degrees of pretilt, along with an effective internal field and an increased viscosity, could explain all the observations. One might have anticipated that broad distributions of length scales, internal fields, pretilt angles, and viscosities would have been needed to fit the data, especially if one works from the hypothesis of strong phase separation during polymerization, which we do not. From that hypothesis, the approach to the data analysis might then have been to assume that the smearing of the Frederiks transition threshold was due to a broad distribution of length scales and pretilt angles for the different compartments of nematic. However, we found such complex data analysis unjustified. The dynamic data, especially for the 125 μm cell, also support the concept of a single mean length scale with only a narrow distribution about the mean. Other more complex interpretations of a single relaxation time are also possible, such as a broad distribution of length scales with an exactly compensating set of viscosities to recover a single exponential relaxation time for the sample, but this again seems unlikely.

We have tried here to outline one consistent approach to understanding gelled nematics based on a homogeneous model without phase separation. This seems to give results indicating that the gelled nematic is accurately described by a small set of parameters that may be amenable to analysis in terms of a simple model of the interacting gel network and nematic phase. To further test this picture will surely require more experiments.

We thank M. Boyden for providing us with the polymer materials, and Robert Pelcovits for discussions of this work and related theories. This research was supported by the National Science Foundation, through Grant No. DMR-9415656 at Brandeis University, and through NSF Science and Technology Center (ALCOM) at Kent State University.

[1] J. W. Doane, in *Liquid Crystals—Applications and Uses*, edited by B. Bahadur (World Scientific, Singapore, 1990), Vol. 1.

[2] R. A. M. Hikmet, J. Appl. Phys. **68**, 4406 (1990).

[3] R. A. M. Hikmet and R. Howard, Phys. Rev. E **48**, 2752 (1993).

[4] H. Gruler, T. Scheffer, and G. Meier, Z. Naturforsch. A **27**, 966 (1972).

[5] H.J. Deuling, in *Solid State Physics: Advances in Research and Applications* (Academic Press, New York, 1978), Vol. 14.

[6] F. -J. Bock, H. Kneppe, and F. Schneider, J. Phys. Chem. **93**, 3848 (1989).

[7] S. Götz, W. Stille, G. Strobl, and H. Scheuermann, Macromolecules **26**, 1520 (1993).